International Journal of Energy
ISSN: 2957-9473 | Vol. 2, No. 1, 2023

Analysis of spatiotemporal distribution of methane column concentration and emission source in permafrost area of Northeast China based on AIRS data

Zhichao Xu [1,2,*], Yunshan Chen [3], Wei Shan [2,*], Yuexing Wu [1]

[1] National Demonstration Center for Experimental Civil Engineering Education, Hunan City University, Yiyang, 413002, China;
[2] Field Scientific Observation and Research Station of the Ministry of Education-Geological Environment System of Permafrost Area in Northeast China, Northeast Forestry University, Harbin, 150040, China;
[3] College of Architecture & Urban Planning, Hunan City University, Yiyang, 413002, China.

[*] **Corresponding author**: Zhichao Xu (Email: xzc@nefu.edu.cn), Wei Shan (Email: shanwei@nefu.edu.cn)

Abstract: Northeast China has the largest high-latitude permafrost distribution zone in China. With the intensification of global warming, the carbon stored in the permafrost will gradually thaw and release in the form of methane gas to air, thus increasing the methane column concentration in the near-surface troposphere. However, at present, the spatiotemporal distribution and emission source of methane column concentration in the near-surface troposphere are not clear. In this paper, using the AIRS (Atmospheric Infrared Sounder) remote sensing data from Aqua satellite, we analyzed the distribution and change trend of the methane column concentration in the near-surface troposphere in Northeast China from 2003 to 2021, and combined with the national meteorological and field monitoring data, we studied the emission mechanism and emission source of surface methane in the permafrost area of Northeast China. Study results show that: the permafrost zone in Northeast China has a high methane emission capacity in four seasons, and the methane column concentration shows a significant double-peak seasonal variation. The first peak appears in summer (June to August) and the maximum appears in August, the second peak appears in winter (December to February) and the maximum appears in December. However, the maximum average growth rate of near-surface methane column concentration in Northeast China appeared in spring (5.378ppbv/a), the reason is that the carbon stored under the permafrost is gradually exposed and released in the form of methane. The emission sources include microbial action, methane transported by wetland groundwater, geological methane (metastable methane hydrate, steady-state methane hydrate and thermogenic methane produced in the deep underground or coal seams) stored in frozen layer. The study provides data and technical support for the estimation of carbon emissions in permafrost areas in Northeast China.

Keywords: Northeast China; Airs; Methane column concentration; Spatiotemporal distribution.

1. Introduction

Northeast China permafrost area is located at the southern edge of the Eurasian continuous permafrost area. It is the largest high-latitude permafrost area in China. The permafrost layer has high temperature, thin thickness and unstable thermal state, and is vulnerable to external environment, climate and human factors. The mean annual average temperature (MAAT) growth in Northeast China is higher than that of the global MAAT growth, the temperature rise in the Great and Small Xing'an Mountains in the north is the largest [3-5]. The study results show that since 1980, the continuous permafrost area in China has decreased from 70%~80% to 30%~50%, and the permafrost area in Northeast China has decreased from 3.9×105km2 to 2.4×105km2 [6,7]. The degradation of permafrost is characterized by the gradual increase of active layer thickness. The degradation mode of permafrost includes simultaneous degradation of upper and lower layers and interlayer partial degradation, among which the lower limit rising speed is higher than the upper limit falling speed [8,9]. With the gradual degradation of the permafrost, a large amount of carbon stored in the permafrost will be gradually released, and the permafrost accounts for about 25% of the land in the northern hemisphere ((22±3)×106km2), containing about 1700Gt (1Gt=1015g) of carbon, almost twice the current atmospheric carbon, and methane is an important form of carbon emissions in permafrost regions . In addition to methane produced by methanogens in wetlands, the ancient carbon stored in permafrost will also be released in the form of methane. At present, scholars have found the presence of methane hydrate in Mohe and other areas in Northeast China [11,12]. The study shows that the total reserves of methane hydrate stable zone in permafrost area of China are about 2.995×1012m3 to 5.081×1012m3, the best estimate is 4.002×1012m3. The methane hydrate stable zone in the permafrost region of Northeast China, represented by the Mohe basin, has a reserve range of 0.49×1012m3 to 0.79×1012m3.

Permafrost-associated gas hydrates are often assumed to contain ~1% of the global gas-in-place in gas hydrates based on a study published over three decades ago [13,14]. A conservative estimate is that 20 Gt C (2.7×1013 kg CH4) may be sequestered in permafrost-associated gas hydrates if methane were the only hydrate-former. This value is slightly more than 1 % of modern estimates (corresponding to 1600 Gt C to 1800 Gt C) for global gas-in-place in methane hydrates and about double the absolute estimate (11.2 Gt C) made in 1981 [13,14]. However, gas hydrate, a frozen, naturally-occurring, and highly-concentrated form of methane, sequesters significant carbon in the global system and is stable only over a range of low-temperature and moderate-pressure conditions. Gas hydrate is widespread in the sediments of marine continental margins and permafrost areas, locations where ocean and atmospheric warming may perturb the hydrate stability field and lead to release of the

sequestered methane into the overlying sediments and soils. Methane and methane-derived carbon that escape from sediments and soils and reach the atmosphere could exacerbate greenhouse warming [14,15]. Methane hydrate is likely undergoing dissociation now on global upper continental slopes and on continental shelves that ring the Arctic Ocean. Many factors—the depth of the gas hydrates in sediments, strong sediment and water column sinks, and the inability of bubbles emitted at the seafloor to deliver methane to the sea-air interface in most cases—mitigate the impact of gas hydrate dissociation on atmospheric greenhouse gas concentrations though. There is no conclusive proof that hydrate-derived methane is reaching the atmosphere now, but more observational data and improved numerical models will better characterize the climate-hydrate synergy in the future [14-17].

Therefore, it is very important to accurately monitor the spatiotemporal distribution of methane column concentration in the permafrost area of Northeast China. At present, there are three main monitoring methods for atmospheric methane concentration: ground-based, space-based and satellite remote sensing. Satellite remote sensing can provide stable, long time series, wide space area, ground or high altitude three-dimensional atmospheric monitoring information, which can effectively make up for the shortage of near-surface observation [18,19]. Commonly used methane observation satellites include SCIMACHY, GOSAT, AIRS and IASI, and the study shows that AIRS satellites have the highest correlation with ground-based observation in China [20-27]. Therefore, this paper studies the spatiotemporal distribution characteristics of the atmospheric methane column concentration in the permafrost area of Northeast China and analyzes the methane emission sources based on the AIRS satellite observation data, National Meteorological Station data from 2003 to 2021, and the field monitoring results in the study area, and gives the conceptual model of methane emission in the permafrost region finally. It is expected to provide data and technical support for the estimation of methane emissions in the permafrost regions of Northeast China.

2. Introduction of study area and Airs data

From north to south, the permafrost in Northeast China mainly presents continuous permafrost, discontinuous permafrost, sporadic permafrost, isolated patches permafrost. The low-lying wetland and forest vegetation can reduce the heat radiation from the sun to the ground surface, reduce and block the transfer of atmospheric heat to the surface permafrost layer, provide good storage conditions for the permafrost layer, and delay the degradation of permafrost (Figure 1). In this paper, Northeast China is selected as the study area to analyze the near-surface layer methane column concentration using remote sensing data, and Sunwu county, Heihe city, located at the southern edge of the permafrost region in Northeast China, is selected as the monitoring point for field monitoring.

The satellite data in this paper comes from the atmospheric infrared detector (AIRS) on the Aqua satellite. AIRS uses multi-aperture, ladder infrared grating array spectroscopy technology to observe and analyze the infrared light from the earth's atmosphere and the earth's surface. The infrared spectral area observed by the detector covers 650~2700cm-1, it is divided into 2378 channels. The average of the spectral resolution of AIRS (λ/Δλ) is about 1200, divided into three bands: 3.74~4.61, 6.20~8.22 and 8.80~15.4μm. Covers 7.66μM methane detection zone, AIRS can cover the world twice a day [29,30].

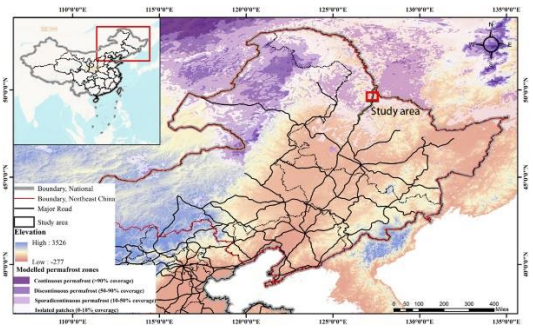
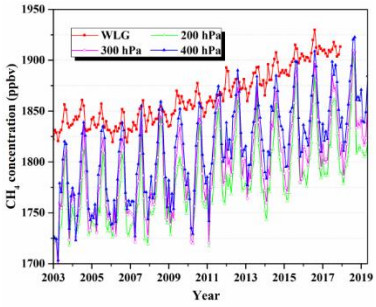
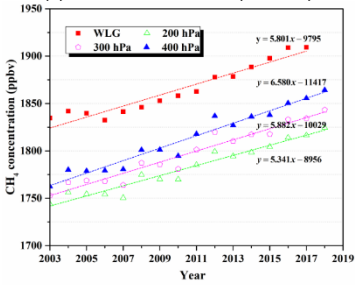


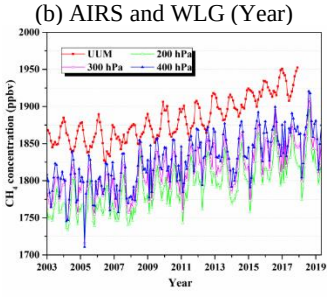
Figure 1. Distribution of permafrost in Northeast China, data from Jaroslav O. et al. (2019)



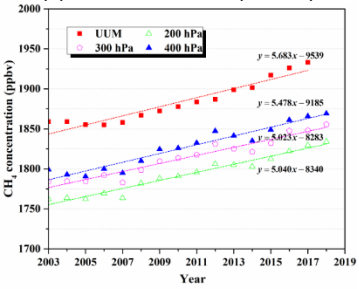
(a) AIRS and WLG (Month)



(b) AIRS and WLG (Year)



(c) AIRS and UUM (Month)



(d) AIRS and UUM (Year)

Figure 2. Curve of methane column concentration in AIRS and atmospheric background station. red line represents atmospheric background station, others represents AIRS.

This paper uses the Airs remote sensing data of methane column concentration from January 2003 to December 2021, and its horizontal resolution is 1°×1°, (URL: https://airs.jpl.nasa.gov/data/get_data). In addition, due to the relatively uneven vertical mixing of methane column concentration in the near-surface troposphere, the range of 1000hPa~200hPa is selected for analysis. In order to verify the reliability of remote sensing data, this paper makes use of the observation data of the global atmospheric background station from 2003 to 2017 at Waliguan (WLG, 100.90°E, 36.28°N, altitude: 3816m) and Ulaan Uul (UUM, 111.09°E, 44.45°N, altitude: 1007m) to carry out quantitative and qualitative comparison and verification of the secondary support products of AIRS (Figure 2).

Pearson correlation analysis of methane column concentration observed value from AIRS and ground-based is carried out through data analysis software SPASS (Table 1). The correlation coefficients of monthly average methane column concentration in WLG are 0.712 (200hPa), 0.721 (300hPa) and 0.747 (400hPa) respectively, and the correlation coefficients of annual average methane column concentration in WLG are 0.968 (200hPa), 0.960 (300hPa) and 0.963 (400hPa) respectively. The correlation coefficients of monthly average methane column concentration in UUM are 0.490 (200hPa), 0.503 (300hPa), 0.542 (400hPa) respectively, and the correlation coefficients of annual average methane column concentration in UUM are 0.963 (200hPa), 0.952 (300hPa), and 0.949 (400hPa) respectively, which have passed the test α= 0.01. Therefore, the methane column concentration from AIRS is significantly positively correlated with the ground-based observed value, and the mutation point is consistent, which can be used for the analysis of methane column concentration distribution characteristics.

Table 1. Correlation coefficients of methane column concentration between AIRS and ground-based observed value

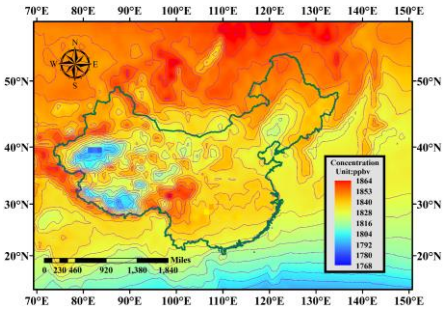
Ground-based observed position	Monthly average			Annual average		
	200 hPa	300 hPa	400 hPa	200 hPa	300 hPa	400 hPa
WLG	0.712	0.721	0.747	0.968	0.960	0.963
UUM	0.490	0.503	0.542	0.963	0.952	0.949
Significance	All passed α=0.01, significant correlation at 0.01 level (two-way)					

3. Results and discussion

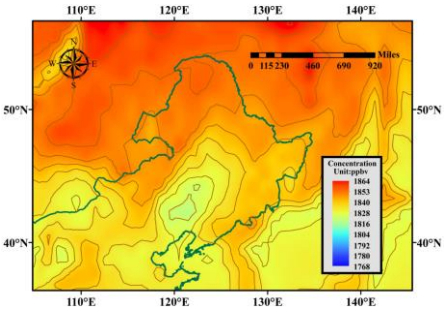
3.1. Spatiotemporal distribution of methane column concentration in Northeast China

This section mainly carries out the analysis of the methane column concentration distribution in the 400hpa near-surface troposphere. The methane column concentration in the near-surface troposphere of China is generally low in the south and high in the north. The high methane column concentration areas in the near-surface troposphere are mainly concentrated in the Northwest, Southwest and Northeast, with the highest value of 1864ppbv (Figure 3a). Among them, the rice planting area in Northeast China accounts for more than 10% of the national total [15,18,25]. However, the methane column concentration in the near-surface troposphere in Northeast China is mainly distributed in the permafrost areas of Great and Small Xing'an Mountains, rather than in the northeast plain area where rice is planted (Figure 3b).

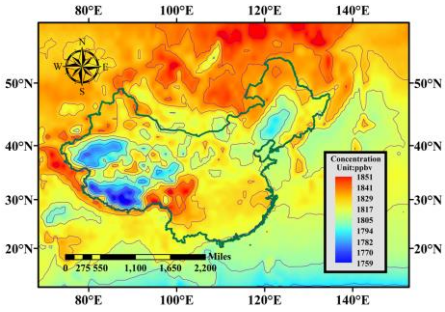
China's near-surface troposphere methane column concentration shows obvious seasonal changes (Figure 3c-f). In spring, the high value of methane column concentration is mainly concentrated in the northeast high-latitude permafrost zone, southwest Sichuan and northern Xinjiang, while the methane column concentration in the northeast plain and Qinghai-Tibet Plateau is relatively low. In summer, the methane column concentration is higher in the middle and high latitudes, but lower in the northwest and south of the Qinghai-Tibet Plateau. In autumn, the methane column concentration in the south is higher than that in the north of China, and the methane column concentration in the southwest is the largest. In winter, the methane column concentration in China is generally low, and the high value is mainly concentrated in the permafrost region of Northeast China. To sum up, Northeast China, especially the high-latitude permafrost region, has a high methane emission capacity in whole year (Figure 3a).



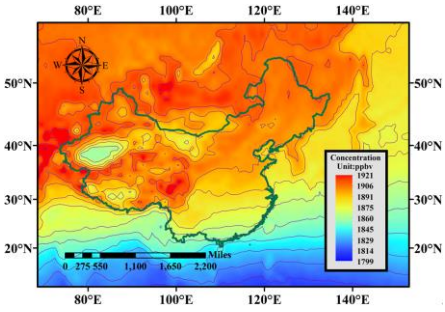
(a) China (Whole year)



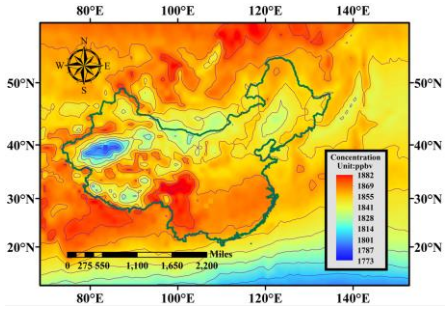
(b) Northeast China (Whole year)



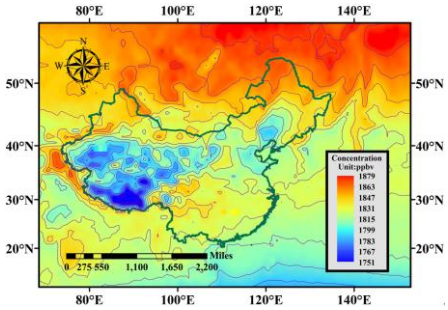
(c) China-Spring (March to May)



(d) China-Summer (June-August)



(e) Autumn (September to November)

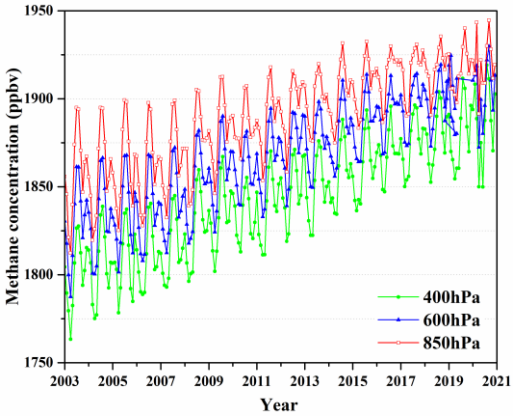


(f) Winter (December to February)

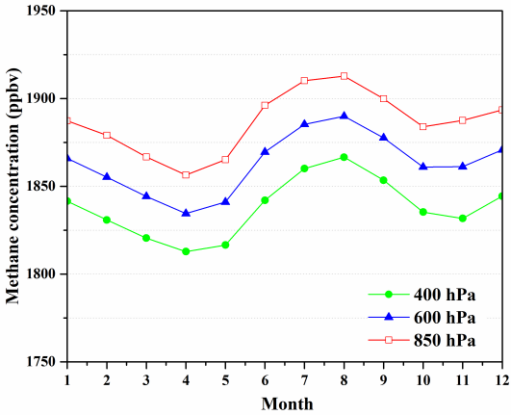
Figure 3. Mean value of methane column concentration distribution in 400hPa near-surface troposphere of China from 2003 to 2021 (Contour line only shows part of China)

It can be seen from the above analysis that the methane emission in Northeast China is an important source of methane emission in the near-surface troposphere of China. The methane column concentration in the near-surface troposphere in Northeast China has gradually increased since 2003 (Figure 4a). The average methane column concentration at 400hPa has increased from 1800ppbv to 1879ppbv, with a linear trend growth rate of 5.401ppbv/a, and the average methane column concentration at 600hPa has increased from 1829ppbv to 1899ppbv, with a linear trend growth rate of 5.112ppbv/a, and the average methane column concentration at 850hPa has increased from 1857ppbv to 1917ppbv, with a linear trend growth rate of 4.626ppbv/a. With the decrease of altitude, the methane column concentration in the near-surface troposphere gradually increases. In addition, the monthly variation of methane column concentration in Northeast China presents a significant double-peak seasonal variation feature (Figure 4b). The first peak appears in summer (June to August), and the maximum appears in August, respectively 1867ppbv (400hPa), 1890ppbv (600hPa), 1913ppbv (850hPa). The second peak appears in winter (December to February), and the maximum appears in December, respectively 1844ppbv (400hPa), 1871ppbv (600hPa), 1894ppbv (850hPa).

Methane column concentration in Northeast China in all seasons shows a gradual upward trend (Figure 5), which is consistent with the change trend of the annually methane column concentration in near-surface troposphere in Northeast China, but the growth rate varies with the seasons. Among them, the growth rate of methane column concentration in the near-surface troposphere in spring is the largest, and the linear trend growth rates are 5.86ppbv/a (400hPa), 6.12ppbv/a (600hPa) and 6.16ppbv/a (850hPa) respectively; the growth rate of methane column concentration in the near-surface troposphere in autumn and winter is the second, and the linear trend growth rates are 6.14ppbv/a (400hPa), 5.83ppbv/a (600hPa) and 5.34ppbv/a (850hPa) respectively in autumn; the linear trend growth rates are 5.73ppbv/a (400hPa), 5.47ppbv/a (600hPa) and 4.89ppbv/a (850hPa) in winter; the growth rate of methane column concentration in the near-surface troposphere in summer is the lowest, and the linear trend growth rates are 4.75ppbv/a (400hPa), 4.03ppbv/a (600hPa) and 3.14ppbv/a (850hPa) respectively.

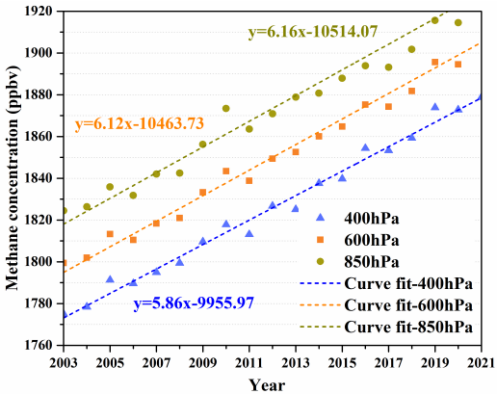


(a) Annually

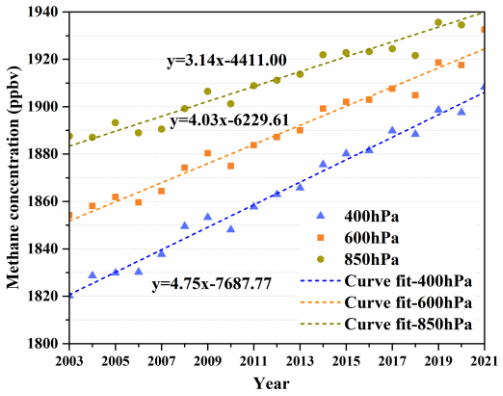


(b) Monthly

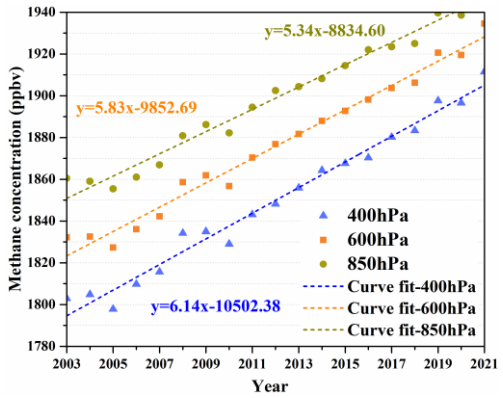
Figure 4. Annually/Monthly average methane column concentration curve of in the near-surface troposphere of Northeast China from 2003 to 2021



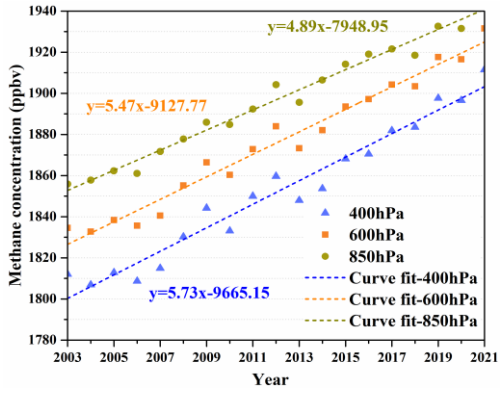
(a) Spring (March to May)



(b) Summer (June to August)



(c) Autumn (September to November)



(d) Winter (December to February)

Figure 5. Seasonal variation of annually mean methane column concentration in the 400hPa near-surface troposphere in Northeast China from 2003 to 2018

3.2. Methane emission sources in permafrost regions of Northeast China

Methane column concentration in the near-surface troposphere of Northeast China shows a rapid growth trend and the increase trend is fastest in spring (Figure 6), while the main growing season of rice in Northeast China is in summer, so rice planting is not the main factor for the increase of methane column concentration in the Northeast China (Rice planting is flooded. Under flooded conditions, decaying plants and other organic substances in the paddy soil are decomposed by methanogenic bacteria to produce a large amount of methane. In addition, rice stalks provide channels for methane release in soil). In addition, the population growth in Northeast China is slow or even more negative, so the impact of population growth (Methane emissions from fossil fuel industry emissions, landfill and wastewater treatment) on methane emissions is relatively small. It is found that the degradation of permafrost regions and oil field development play a major role in the growth of methane column emissions in Northeast China combined with data research and field observation. Northeast China has formed a large area of sedimentary basins through many geological changes during the geological history period, deposited a large amount of carbon (geological methane, etc). After that, it underwent many ice ages to form a cryosphere to completely seal carbon up. However, with the development of global warming, the permafrost region gradually melts, which gradually exposes and releases the carbon stored under the permafrost.



(a) Methane under the ice



(b) Methane in wetland



(c) Methane-containing ice core

Figure 6. Methane released in spring from permafrost areas in Northeast China

The carbon stored in the permafrost will be gradually converted into methane under the action of methanogens. In addition to the role of recent methanogens, the ancient carbon stored in permafrost will also be released in the form of

geological methane (stored during geological time, like methane hydrate). At present, many large oilfields have been found in the Northeast China, including Daqing oilfield, Jilin oilfield, etc., and scholars have found the presence of methane hydrate in Mohe and other areas in Northeast China [30,31]. The total reserves of methane hydrate stable zone in permafrost regions of China are about 2.995×1012m3 to 5.081×1012m3, the best estimate is 4.002×1012m3. The methane hydrate stable zone in the permafrost area of Northeast China, represented by the Mohe, has a reserve range of 0.49×1012m3 to 0.79×1012m3. In addition, Klusman et al. also believe that the microleakage area of methane gas may include all sedimentary basins with oil and gas production processes, and the release process may increase significantly with the increase of global temperature. Therefore, the main sources of atmospheric methane in the permafrost regions of Northeast China include microbial action, methane transported by wetland groundwater, geological methane (metastable methane hydrate, steady-state methane hydrate and thermogenic methane produced in the deep underground or coal seams) stored in frozen layer. Among them, the distribution and proportion of hydrocarbons in the Mohe basin and Sunwu-Jiayin basin are shown in Tables 2 and 3 [34,35].

Table 2. Gas composition of drilling core in Mohe basin

Gas composition	Methane	Ethane	Propane	Isobutane	N-butane	Isopentane	N-pentane
gas concentration / (μL·L-1)	274747.86	11844.48	4296.00	634.32	722.61	208.27	74.49
Content/%	93.92	4.05	1.47	0.22	0.25	0.07	0.03

Table 3. Organic matter abundance of hydrocarbon source rocks in Sunwu-Jiayin basin

Stratum	TOC (%)	Chloroform asphalt A (%)	S1+S2 (mg/g)	Total hydrocarbon (mg/g)
Taiping Forest Farm Group	0.51~1.13 0.89 (7)	0.0071~0.0190.0128 (5)	0.31~0.94 0.55 (7)	
Yong'an Village Group	0.16~4.51 1.33 (23)	0.0045~0.0348 0.0139 (12)	0.06~22.48 2.63 (21)	54.41~76.86 61.89 (3)
Taoqihe Formation	0.21~4.98 1.89 (171)	0.0039~0.1169 0.0261 (49)	0.045~20.468 2.94 (171)	46.3~80.39 61.66 (13)
Ningyuan Village Group	0.10~5.93 1.72 (23)	0.0047~0.0451 0.0249 (2)	0.024~14.012.31 (5)	

3.3. Methane emission mechanism in permafrost degraded areas in Northeast China

In order to further analyze the degradation of permafrost in Northeast China, the data from the National Meteorological Station of Sunwu County, Heihe City, located in the degradation zone of the southern edge of the permafrost region in Northeast China, were selected for analysis, and the seasonal changes of permafrost in the region were analyzed in combination with the high-density resistivity method results of the study area for many years (Figure 7). The monthly average temperature in January of each year in the region is the lowest, with the air temperature and ground temperature reaching -24.5℃ and -26.6℃, and the frozen soil temperature reaching -7.9℃. The monthly average temperature in July is the highest, with the air temperature and ground temperature reaching 23.8℃ and 19.9℃, and the frozen soil temperature reaching 16℃. The whole temperature is in a parabolic shape that increases first and then decreases. The monthly maximum frozen soil depth shows a trend of increasing first, then decreasing and finally increasing. The maximum depth of frozen soil in January to May -gradually increased, and the maximum depth of frozen soil in spring (March to May) reached the maximum (239.0cm) in April and May. The maximum monthly frozen soil depth gradually decreases from May to September and reached the minimum value (12.0cm) in September. The monthly maximum frozen soil depth increased again in October and December, reached the second peak (131cm) in December. It can be seen that the maximum monthly frozen soil depth appeared in spring, which is consistent with the rise season of the methane column concentration in the study area . This is due to the isolation of the frozen surface in permafrost areas, most of the methane cannot be immediately re-leased into the atmosphere in winter. In the thawing season of the following year, the methane is expected to be released over a very short time, thus forming an emission explosion (at this time, the methane concentration at the leakage point is greater than 10,000 ppm, reaching the upper limit of the SKZ1050-CH4 methane handheld detector (Figure 6b), and the igniting gas at the leakage point can form flames with heights of 1.5 m). Therefore, the methane gas concentrations at these points are very high, and the emission pressures are also high.

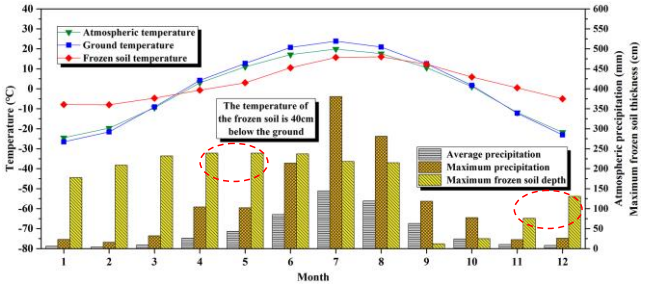


Figure 7. Curve of meteorological data near study area from 1987 to 2021

The high-density resistivity method (HDR) is further used to detect the thickness of permafrost in the study area. The

results show that the area and resistivity of the high resistivity area are continuously decreasing, the thickness of permafrost is gradually thinning, the distribution range is also gradually decreasing, and a large number of methane leakage points are found in the permafrost distribution area (Figure 8c). With the gradual degradation of the permafrost, a large amount of carbon stored in the permafrost will be gradually released, and the permafrost accounts for about 25% of the land in the northern hemisphere ((22±3)×106km2), containing about 1700Gt (1Gt=1015g) of carbon, almost twice the current atmospheric carbon, and methane is an important form of carbon emissions in permafrost regions . Carbon stored in the permafrost layer will gradually transform into methane gas and gradually accumulate in the intermediate unfrozen layer under the surface frozen layer, showing the transformation from "stable organic matter carbon pool" to "metastable methane gas carbon pool", thus accelerating the carbon cycle in the permafrost region.

Combined with the detection results, we finally gave the conceptual model of frozen soil melting and methane emission in the study area. The top layer of the geological structure in the study area is peat soil containing a large amount of soil carbon, the lower layer is frozen soil layer containing sand and mudstone, and the frozen soil layer contains a certain amount of methane (including recent microbial action in active layer, methane transported by wetland groundwater in intermediate unfrozen layer, and geological methane (like methane hydrate, etc) stored in deep frozen layer) (Figure 8ab). With the degradation of frozen soil, this part of methane will be released rapidly.

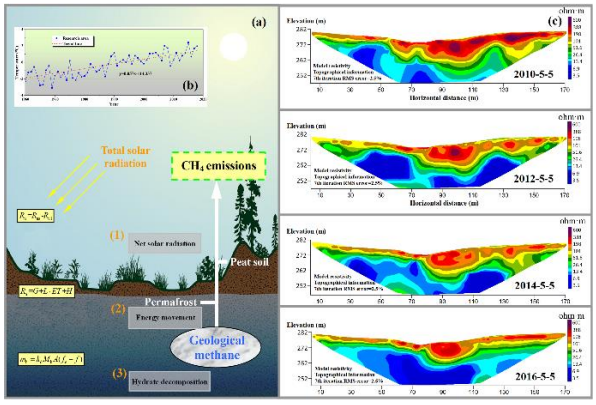


Figure 8. Methane emission mechanism and frozen soil change in the study area

The heat in the soil mainly comes from solar radiation. After being absorbed by the atmosphere and reflected by the ground, the net solar radiation entering the ground is Rn, see Equation 1. Net radiation reaching the surface flows into or out of the soil, forming the soil heat flux. One part is used to heat soil and air (sensible heat), which will further accelerate the thawing of frozen soil, and the other part is used for soil and crop transpiration (latent heat), where the energy balance equation can be expressed as Equation 2. When the frozen soil is disturbed and thawed, moving pore water will form in the soil and continue to affect the methane hydrate in the lower part, resulting in the decomposition of methane hydrate to generate methane gas. Kim kinetic decomposition model can be selected to describe the decomposition of methane hydrate, as shown in Equation 3.

$$R_n = R_{ns} - R_{n1} \quad (1)$$

$$R_n = G + L \cdot ET + H \quad (2)$$

$$m_h = k_d M_h A(f_e - f) \quad (3)$$

Where, Rn is net solar radiation, Rns is net short-wave radiation, Rn1 is net long-wave radiation, G is soil heat flux, L is potential vaporization heat, ET is evapotranspiration, L•ET is latent heat flux, H is sensible heat flux; mh is the methane hydrate decomposition rate, kg/(m3•s); Mh is the molar mass of methane hydrate, kg/mol; A is the specific surface area of reaction m2; fe is the phase equilibrium fugacity, f is the local gas fugacity, MPa, expressed by phase equilibrium pressure and local pressure respectively; kd is the decomposition rate of methane hydrate.

4. Conclusions

This paper uses the AIRS remote sensing data from Aqua satellite to analyze the distribution and change trend of the total methane column concentration of the near-surface troposphere in Northeast China from 2003 to 2021, analyze the source and mechanism of surface methane emission in the permafrost region of Northeast China combined with the National Meteorological data and the field monitoring results in the study area, and draws the following conclusions:

Overall, from 2003 to 2021, the near-surface troposphere methane column concentration in China was low in the south and high in the north, and the high-value areas of methane column concentration mainly appeared in the Northeast China, et al, especially the high-latitude permafrost zone, it has a high methane emission capacity in four seasons. The methane column concentration in the near-surface troposphere presents a significant double-peak seasonal variation feature. The first peak appears in summer (June to August), the maximum appears in August, the second peak appears in winter (December to February), and the maximum appears in December. From 2003 to 2021, China's near-surface troposphere methane column concentration showed an overall upward trend. The average growth rate in Northeast China was relatively large, reaching 4.626ppbv/a, and the annual average value of near-surface troposphere (400hPa) methane column concentration increased from 1800ppbv to 1879ppbv, and the methane column concentration gradually increased with the decrease of height. The growth rate of methane column concentration in the near-surface troposphere of Northeast China varies with seasons. On the whole, the average growth rate of methane column concentration in spring is the largest (5.378ppbv/a), followed by the average growth rate of methane column concentration in autumn (5.127ppbv/a) and winter (4.804ppbv/a), and the average growth rate of methane column concentration in summer is the lowest (2.860ppbv/a). With the development of global warming, the permafrost regions in Northeast China are gradually degraded, and the carbon stored under the permafrost is gradually exposed and released in the form of methane (microbial action, methane transported by wetland groundwater, geological methane (metastable state methane hydrate, steady state methane hydrate and thermogenic methane produced in the deep underground or coal seams)), and the release rate is the fastest in spring. This is also one of the main reasons for the rapid increase of methane column concentration in spring in Northeast China.

Acknowledgments

We thank the National Natural Science Foundation of China (Grant No. 41641024) and Science and the Technology

Project of Heilongjiang Communications Investment Group (Grant No. JT-100000-ZC-FW-2021-0182) for providing financial support and the Field scientific observation and research station of the Ministry of Education-Geological environment system of permafrost area in Northeast China (MEORS-PGSNEC).

References

[1] Wei Z., Jin H.J., Zhang J.M., et al. Prediction of permafrost change in northeast China under climate change. Science China: Earth Science, 2011, 41: 74-84.

[2] Ren G.Y., Guo J., Xu M.Z., et al. Climate changes of China's mainland over the past half century. Acta Meteorologica Sinica, 2005, 63: 942-956.

[3] He W., Bu R.C., Xiong Z.P., et al. Characteristics of temperature and precipitation in Northeastern China from 1961 to 2005. Acta ecologica sinica, 2013, 33: 519-531.

[4] Wei Z., Jin H.J., Luo C.X., et al. Characteristics of atmospheric environmental changes of permafrost in northeastern China in 50 years. Journal of Lanzhou University (Natural Science), 2008, 44: 39-42.

[5] Guo J.T., Han F.L., Hu Y.M., et al. Ecological characteristics of vegetation and their responses to permafrost degradation in the north slope of Great Khingan Mountain valley of northeast China. Acta Ecologica, 2017, 37: 6552-6561. (In Chinese)

[6] Shan W., Xu Z.C., Guo Y., et al. Geological methane emissions and wildfire risk in the degraded permafrost area of the Xiao Xing'an Mountains, China[J]. Scientific Reports, 2020, 10: 21297.

[7] Zhao L., Sheng Y. Permafrost survey manual[M]. Beijing: Science Press, 2000.

[8] Guo Y., Shan W., Zhang C.C., et al. Monitoring of permafrost degradation along the Bei'an-Heihe expressway in China. Bulletin of Engineering Geology and the Environment, 2020, 16: 1-10.

[9] Zhao D.D., Liu J.F., Liu J.P., et al. A review of main studies on permafrost degradation in Northeast China. Science Technology and Engineering, 2022, 22: 13151-13161. (In Chinese)

[10] Tarnocai C., Canadell J.G., Schuur E.A., et al. Soil organic carbon pools in the northern circumpolar permafrost region. Global Biogeochemical Cycles, 2009, 23: 1-11.

[11] Zhao X. M., Deng J., Rao Z., et al. Shallow gas characteristics in Mohe Basin,Northeast China and its significance to gas hydrate formation. Acta Petrolei Sinica, 2018, 39: 266-277. (In Chinese)

[12] Wang X., Pan L., Lau H.C., et al. Reservoir volume of gas hydrate stability zones in permafrost regions of China. Applied Energy, 2018, 225: 486-500.

[13] Farahani M. V., Hassanpouryouzband A., Yang J., et al. Insights into the climate-driven evolution of gas hydrate-bearing permafrost sediments: Implications for prediction of environmental impacts and security of energy in cold regions. Rsc Advances, 2021, 11: 14334-14346.

[14] Farahani M. V., Hassanpouryouzband A., Yang J., Tohidi B. Development of a coupled geophysical–geothermal scheme for quantification of hydrates in gas hydrate-bearing permafrost sediments. Physical Chemistry Chemical Physics, 2021, 23: 24249-24264.

[15] Ruppel C.D., Kessler J. D. The interaction of climate change and methane hydrates. Reviews of Geophysics, 2017, 55: 126-168.

[16] Ruppel C. Permafrost-associated gas hydrate: is it really approximately 1% of the global system?. Journal of Chemical & Engineering Data, 2015, 60: 429-436.

[17] Archer D., Buffett B., Brovkin V. Ocean methane hydrates as a slow tipping point in the global carbon cycle. Proceedings of the National Academy of Sciences of the United States of America, 2009, 106: 20596-20601.

[18] Zhang X.Y., Zhang P., Fang Z.Y., et al. The progress in trace gas remote sensing study based on the satellite monitoring. Meteorological monthly, 2007, 33: 1-14.

[19] Zhang S.H., Xie, B., Zhang H., et al. The spatial-temporal distribution of CH4 over globe and East Asia. China Environmental Science, 2018, 38: 4401-4408. (In Chinese)

[20] Zhang X., Zhang X., Zhang L., et al. Accuracy comparison of monthly AIRS, GOSAT and SCIAMACHY data in monitoring atmospheric CH4 concentration. International Conference on Geoinformatics, 2013: 1-4.

[21] Zhang X.Y., Bai W.G., Zhang P., et al. Spatiotemporal variations in mid-upper tropospheric methane over China from satellite observations. Chinese Science Bulletin, 2011, 56: 2804-2811. (In Chinese)

[22] Wang H.M., Li J.T., Zhang Y., et al. Spatial and temporal distribution of near-surface methane concentration over China based on AIRS observations. Journal of Remote Sensing, 2015,19: 827-835. (In Chinese)

[23] Yang Q., Guan L., Liang M., et al. Changes of CH4 concentrations obtained by ground-based observations at five atmospheric background stations in China. Environmental Science & Technology, 2018, 41: 1-7. (In Chinese)

[24] Setyanto P., Rosenani A. B., Makarim A. K., et al. Soil controlling factors of methane gas production from flooded rice fields in Pati District, Central Java. Indonesian Journal of Agricultural Science, 2016, 3: 1-11.

[25] Pedersen E.P., Elberling B., Michelsen A. Seasonal variation in methane fluxes from sedimentary basins to the atmosphere: Results from chamber measurements and modeling of transport from deep sources. Journal of Geophysical Research, 2000, 105: 661-670.

[26] Zhang F.G., Sun Z.J., Yang Z.B., et al. Geochemical Investigation of Gas Hydrate in the Permafrost Area. China. Bulletin of Mineralogy, Petrology and Geochemistry, 2019, 38: 1-11.

[27] Kim H.C., Bishnol P.R., Heidemann R.A., et al. Kinetic of methane hydrate decomposition. Chemical Engineering Science, 1987, 42: 1645-1653.

[28] Jaroslav O., Sebastian W., Annett B., et al. Northern Hemisphere permafrost map based on TTOP modelling for 2000-2016 at 1 km2 scale. Earth-Science Reviews, 2019, 193: 299-316.

[29] Setyanto P., Rosenani A.B., Makarim A.K., et al. Soil controlling factors of methane gas production from flooded rice fields in Pati District, Central Java. Indonesian Journal of Agricultural Science, 2016, 3: 1-11.

[30] Xu Z.C., Shan W., Guo Y., et al. Swamp wetlands in degraded permafrost areas release large amounts of methane and may promote wildfires through friction electrification. Sustainability, 2022, 14L: 9193.

[31] Zhang F.G., Tang R.L., Yang Z.B., et al. Geochemical Investigation and Prospective Evaluation of Natural Gas Hydrates in the Permafrost of Mohe Basin. Geoscience, 2018, 32: 1003-1011. (In Chinese)

[32] Wang X., Pan L., Lau H.C., et al. Reservoir volume of gas hydrate stability zones in permafrost regions of China. Applied Energy, 2018, 225: 486-500.

[33] Klusman R.W., Leopold M.E., Michelsen A., et al. Seasonal variation in methane fluxes from sedimentary basins to the atmosphere: Results from chamber measurements and modeling of transport from deep sources. Journal of Geophysical Research, 2000, 105: 661-670.

[34] Deng J., Zhao X.M., Lu C. Discussion on the characteristics, origin and source of physically adsorbed hydrocarbons in the scientific drilling well (MK-1) in the Mohe Basin, Northeast China. Mineral Deposits, 2012, 31: 1091-1092. (In Chinese)

[35] Zhao X.M., Deng J., Rao Z., et al. Abnormalities of stable carbon and hydrogen isotopes of methane in the Mohe Basin, Northeast China and mechanisms of isotopic change. Earth Science Frontiers, 2019, 26: 231-237. (In Chinese)